

APR 13 1955 RECD

CONFIDENTIAL

Copy /
RM SL55D19

CLASSIFICATION CANCELLED

AUTHORITY NASA TECHNICAL PUBLICATION
ANNOUNCEMENTS NO.

NACA

CLASSIFICATION CHANGE

Unclassified
authority of *NASA Memo. Oct 5-2-23 / 15/64 H-Maines*
changed by *M.R. [unclear]* Date *6-7-23*

RESEARCH MEMORANDUM

for the

U. S. Air Force

AERODYNAMIC CHARACTERISTICS OF A 0.04956-SCALE MODEL OF

THE CONVAIR F-102A AIRPLANE AT TRANSONIC SPEEDS

By Kenneth E. Tempelmeyer and Robert S. Osborne

Langley Aeronautical Laboratory
Langley Field, Va.

~~CLASSIFIED DOCUMENT~~

This material contains information affecting the National Defense of the United States within the meaning of the espionage laws, Title 18, U.S.C., Sections 793 and 794, the transmission or revelation of which in any manner to an unauthorized person is prohibited by law.

NATIONAL ADVISORY COMMITTEE FOR AERONAUTICS

WASHINGTON

APR 11 1955

FILE COPY

To be returned to
the files of the National
Advisory Committee
for Aeronautics
Washington, D. C.

CONFIDENTIAL

14

CONFIDENTIAL

NATIONAL ADVISORY COMMITTEE FOR AERONAUTICS

RESEARCH MEMORANDUM

for the

U. S. Air Force

AERODYNAMIC CHARACTERISTICS OF A 0.04956-SCALE MODEL OF

THE CONVAIR F-102A AIRPLANE AT TRANSONIC SPEEDS

By Kenneth E. Tempelmeyer and Robert S. Osborne

SUMMARY

Tests have been conducted in the Langley 8-foot transonic tunnel on a 0.04956-scale model of the Convair F-102A airplane which employed an indented and extended fuselage, cambered wing leading edges, and deflected wing tips. Force and moment characteristics were obtained for Mach numbers from 0.60 to 1.135 at angles of attack up to 20° . In addition, tests were made over a limited angle-of-attack range to determine the effects of the cambered leading edges, deflected tips, and a nose section with a smooth area distribution.

Fuselage modifications employed on the F-102A were responsible for a 25-percent reduction in the minimum drag-coefficient rise between the Mach numbers of 0.85 and 1.075 when compared with that for the earlier versions of the F-102. Although the wing modifications increased the F-102A subsonic minimum drag-coefficient level approximately 0.0020, they produced large decreases in drag at lifting conditions over that for the original (plane-wing) F-102. The F-102A had 15 to 25 percent higher maximum lift-drag ratios than did the original F-102. The F-102A had about 15 percent lower maximum lift-drag ratios at Mach numbers below 0.95 and slightly higher maximum lift-drag ratios at supersonic speeds when compared with those ratios for an earlier modified-wing version of the F-102. Chordwise wing fences which provided suitable longitudinal stability for the original F-102 were not adequate for the cambered-wing F-102A. The pitching-moment curves indicated a region of near neutral stability with possible pitch-up tendencies for the F-102A at high subsonic Mach numbers for lift coefficients between about 0.4 and 0.5.

CONFIDENTIAL

INTRODUCTION

At the request of the U. S. Air Force, an investigation has been made in the Langley 8-foot transonic tunnel to determine the stability, control, and performance characteristics of a 1/20-scale model of the Convair F-102 airplane. Results of the initial tests, published in references 1 and 2, indicated that the original configuration had high transonic zero-lift drag, high drag due to lift, and high drag due to trim. In subsequent tests, it was indicated that the transonic zero-lift drag of the original configuration could be reduced by employing modifications based on the area-rule concept such as fuselage indentation (ref. 3) and afterbody extensions (ref. 4). It was also found that the drag due to lift and drag due to trim could be reduced by respectively cambering the wing leading edge and deflecting the wing tips to effectively increase the elevator control surface area (ref. 5).

On the basis of the results just described and results obtained in other NACA facilities (refs. 6 and 7, for example), the Convair F-102 was redesigned by the contractor (with the collaboration of the NACA) to incorporate cambered wing leading edges, deflected wing tips (trailing edges up), and an indented and extended fuselage. The redesigned airplane has been designated the F-102A. In order to determine the aerodynamic characteristics of the redesigned configuration, a 0.04956-scale model of the F-102A has been tested with controls undeflected in the Langley 8-foot transonic tunnel at Mach numbers from 0.60 to 1.135 at angles of attack up to 20°. In addition, in order to separate the effects of the leading-edge camber and deflected tips on the minimum drag of the redesigned configuration, the model was tested first with undeflected tips and then with undeflected tips and no leading-edge camber for lift coefficients up to about 0.2. Also, to ascertain possible drag reductions due to improving the cross-sectional distribution of the forward portion of the model, a configuration employing a smooth parabolic nose (without canopy) was tested at lift coefficients up to 0.2. The results are presented herein.

The results of tests of the 0.04956-scale model of the F-102A at a Mach number of 1.41 are presented in reference 8 and free-flight zero-lift drag results of a 1/5-scale model with plane wing leading edges and tips are available in reference 9.

SYMBOLS

- b wing span, in.
 \bar{c} mean aerodynamic chord, in.

C_D	drag coefficient adjusted to free-stream static pressure at model base, D/qS
C_L	lift coefficient, L/qS
$C_{L(L/D)_{max}}$	lift coefficient for maximum lift-drag ratio
$\partial C_L / \partial \alpha$	lift-curve slope per degree, averaged from $\alpha = 0^\circ$ over approximately linear portion of curve
C_m	pitching-moment coefficient, $\frac{M_{cg}}{qS\bar{c}}$
$\partial C_m / \partial C_L$	static-longitudinal-stability parameter, averaged from $C_L = 0$ over linear portion of curve
D	drag adjusted to free-stream static pressure at model base, lb
L	lift, lb
$(L/D)_{max}$	maximum lift-drag ratio
M	free-stream Mach number
M_{cg}	pitching moment about center-of-gravity location, in-lb
P_b	base pressure coefficient, $\frac{P_b - P_o}{q}$
P_b	static pressure at model base, lb/sq ft
P_o	free-stream static pressure, lb/sq ft
q	free-stream dynamic pressure, lb/sq ft
S	total wing area, sq ft
α	angle of attack of wing chord plane with no leading-edge droop, deg

APPARATUS AND METHODS

Tunnel and Model Support System

The tests were conducted in the Langley 8-foot transonic tunnel which is a dodecagonal slotted-throat, single-return wind tunnel designed

to obtain aerodynamic data through the speed of sound while minimizing the usual effects of blockage. The tunnel operates at approximately atmospheric stagnation pressures. Details of test-section design and flow uniformity are available in reference 10.

The model was attached to a sting support through an electrical strain-gage balance located inside the fuselage. The sting support was cylindrical for 2.8 base diameters downstream of the model base and was fixed on the tunnel axis by two sets of struts projecting from the tunnel walls. Angled couplings in the sting were employed to maintain the model position near the tunnel center line at all angles of attack.

Model

The 0.04956-scale model of the Convair F-102A airplane used in this investigation was supplied by the contractor. The basic configuration, which included an indented and extended fuselage and a wing with cambered leading edges and deflected tips, is shown in figure 1. Its dimensional details are presented in figure 2 and table I.

The basic F-102A wing was derived from a plane 60° delta wing employing modified NACA 0004-65 streamwise airfoil sections (see ref. 1) by extending the leading edge approximately 4.1 percent of the mean aerodynamic chord and conically cambering the outboard 6.37 percent of the local semispan. The amount of camber was equal to the theoretical value required to support an elliptical span load distribution at a lift coefficient of 0.15 near a Mach number of 1.0. The camber was identical with the modification 6 camber of reference 5 with the exception of a small increase in leading-edge radius and an increase in leading-edge sweep angle from 60° to 60.14° . The trailing edge of the wing tips outboard of the 82-percent-semispan station was deflected upward 10° about the elevator hinge line extended.

Details of the F-102A basic-wing plan form, leading-edge camber, and deflected tips are given in figure 3. The wing was constructed with a steel core covered with a tin-bismuth surface. Aluminum-alloy leading edges and steel tips were removable which allowed the F-102A model to be tested with the plane uncambered leading edges and undeflected tips used on the models of references 1 to 4. Chordwise fences (ordinates in table II) were installed at the 66-percent-semispan station on the cambered wing. There were no fences on the plane-wing configurations.

The fuselage was equipped with twin ram-jet inlets which were closed for these tests by means of faired plugs. (See fig. 2.) The F-102A fuselage was obtained by completely redesigning the original F-102 rearward of the canopy. The fuselage was extended about 13 percent

10
0
10
0
00
0
00
0
00
0

and, using the supersonic area-rule concept (ref. 11), it was indented for the wing and tail in a manner to give a smooth total area distribution at a design Mach number of 1.2. The supersonic area rule states that the area to be removed from the body is the normal component of the average area intersected outside the body by several planes tangent to the design Mach cone. The $M = 1.2$ area distribution derived from a number of equally spaced cuts and the resulting area distribution for $M = 1.0$ are presented in figure 4. The increased body length necessitated moving the wing and vertical tail rearward to provide approximately the same static margin. A comparison of the F-102A and F-102 is shown in figure 5 and their corresponding area distributions are compared in figure 4.

A nose section, evolved from parabolic segments, which eliminated the rapid increase of cross-sectional area due to the canopy and inlets was tested on a configuration with plane wing leading edges and undeflected tips. The parabolic nose is compared with the F-102A nose in figure 6. Their area distributions are given in figure 4.

The various configurations tested and their plan-form characteristics are listed in table III.

Measurements and Accuracy

Normal force, axial force, and pitching moment were measured with the internal strain-gage balance and reduced to lift, drag, and pitching-moment coefficients based on the actual wing area and mean aerodynamic chord of the configuration (table III). The pitching-moment coefficients were obtained for a center-of-gravity location of 29.6 percent of the mean aerodynamic chord (27.5 percent for the original plane leading-edge plan form) and 4.5 percent of the mean aerodynamic chord above the wing chord plane. Accuracies of the coefficients are estimated to be within the following limits for lift coefficients up to at least 0.4:

C_L	± 0.005
C_D	± 0.001
C_m	± 0.001

The angle of attack was determined within 0.15° by a pendulum-type inclinometer located in the sting support and from a calibration of sting and balance deflection due to model loads. The variation of test section Mach number in the vicinity of the model did not exceed 0.003 at subsonic speeds and 0.010 at a Mach number of 1.135.

Base pressure coefficients were obtained from an orifice located well inside the model forward of the plane of the base. The accuracy of the base pressure coefficients is estimated to be within 0.005.

Tests

All configurations were tested at Mach numbers from 0.60 to 1.135. As previously mentioned, all tests were made with the ducts faired closed. The angle-of-attack range for the basic F-102A configuration varied from 0° to approximately 20° . The additional three configurations with (1) undeflected tips, (2) plane leading edges and undeflected tips, and (3) plane leading edges, undeflected tips, and a parabolic nose were tested at angles of attack from 0° to about 4° to define the minimum drag.

A range of test Reynolds numbers based on the wing mean aerodynamic chords is shown in figure 7. The average Reynolds number was of the order of 4.6×10^6 .

Corrections

Subsonic boundary interference is minimized by the slotted test section, and no corrections for this interference have been applied. The effects of supersonic boundary-reflected disturbances were reduced by testing the model several inches from the tunnel center line. However, it is possible that these disturbances caused small errors in the drag and pitching-moment measurements at Mach numbers of 1.075 and 1.135. It is believed that these errors have been minimized by judicious fairing of the data plotted against Mach number in the summary and analysis plots and that indicated trends are free of boundary-reflected disturbances.

No sting interference corrections have been applied to these data. The drag data have been adjusted to an assumed condition of free-stream static pressure acting over the model base.

RESULTS

All tests were made with the ducts closed and the data have been adjusted to represent free-stream static pressure at the model base using the base pressure coefficients shown in figure 8.

Force and moment characteristics of the basic F-102A model are presented in figure 9. The data for the F-102A configurations with undeflected tips; with plane leading edges and undeflected tips; and with plane leading edges, undeflected tips, and a parabolic nose are given in figures 10, 11, and 12, respectively, with a summary figure showing the effects of these modifications on the minimum drag coefficient in figure 13.

The basic F-102A model has been compared in summary and analysis figures 14 to 17 with the original F-102 with ducts closed (ref. 4) and the modified-wing F-102 model with ducts open (ref. 5). The internal drag has been removed from the data of reference 5. Due to scale deviations of the models of references 4 and 5, it was necessary to apply a correction, obtained by the method presented in reference 12, to their drag data. This correction, as presented in reference 5, has been used in the preparation of these figures.

Shock formations near the wing trailing edge as indicated by schlieren photographs are compared for the F-102A and the F-102 at a Mach number of 1.0 in figure 18.

Sliding scales have been employed in many figures and care should be taken in selecting the zero axis for each curve.

DISCUSSION

Drag Characteristics

Minimum drag.- The drag polars for the basic F-102A model indicated that the minimum drag occurred at a lift coefficient of about 0.05 at most Mach numbers and the minimum incremental-drag-coefficient increase was approximately 0.015 between Mach numbers of 0.85 and 1.075 (fig. 9(a)). The effects of the cambered leading edges as well as the deflected tips on the minimum drag are shown in figure 13. These combined wing modifications employed on the F-102A were responsible for increasing the minimum drag-coefficient level about 0.0020 throughout the speed range. The cambered leading edges were responsible for about 0.0015 of this increase and the deflected tips produced the additional 0.0005.

The parabolic nose which eliminated the unfavorable area build-up of the canopy and inlets was responsible for an additional reduction in the drag-rise coefficient of 0.0017 at a Mach number of 1.075 (fig. 13). This reduction was primarily due to the improvement of area distribution over the forward portion of the fuselage (see fig. 4) which reduced the induced velocities in this critical area region. The improvement in area distribution was largely due to removal of the canopy (see fig. 6) which would be impractical on the full-scale airplane. However, moving the inlets rearward would result in an improvement in the nose-section area distribution and some drag reduction could be expected from such a modification even with the canopy installed.

Comparing the F-102A with the modified-wing F-102 (ref. 5) indicates that the effect of the area-rule body modifications in combination with the wing with cambered leading edges and deflected tips was to reduce the

drag rise about 25 percent at a Mach number of 1.075 (fig. 14). The difference in subsonic drag levels is primarily due to the increase in surface area and hence skin friction for the F-102A. A similar drag-rise reduction due to body modifications in combination with the plane wing may be seen by comparing the F-102A with plane leading edges and 0° tips (fig. 13) with the original F-102 of reference 4 (fig. 14). Schlieren photographs (fig. 18) show the effects of body modifications (in the presence of the plane wing) on the shock field near the wing trailing edge at a Mach number of 1.0. These photographs taken in the vertical plane do not reveal the complete flow phenomena associated with the area-rule modifications since the supersonic area rule is based on shock-formation reductions in every plane; however, it appears that the body modification employed on the F-102A has reduced the strength of the shock field and resulted in the above-mentioned drag-rise decrease. It should be noted that the frontal area of the F-102A was not reduced, and that this drag-rise reduction was due to the increased body fineness ratio and body indentation with its attendant reduction of wing-body interference.

A comparison of the minimum drags for the F-102A and the original F-102 of reference 4 indicated the expected drag penalty from the wing modifications on the F-102A at low Mach numbers (fig. 14). At Mach numbers above 0.95, the F-102A body modifications reduced the drag-coefficient level an average of 0.004.

Drag at lifting conditions.- As stated in reference 5 and illustrated in figure 15, the cambered leading edges applied to the original F-102 produce large reductions in drag due to lift. The leading-edge camber reduces leading-edge separation and hence increases the suction forces over the leading edge. Comparison of the basic F-102A model with the modified-wing F-102 of reference 5 (fig. 15) indicated that the F-102A body modifications had an adverse effect on the drag at lifting conditions (at subsonic Mach numbers). For example, the difference in the minimum drag-coefficient levels (near $C_L = 0$) for these two configurations at subcritical speeds is about 0.0012 (fig. 14) whereas at a lift coefficient of 0.3 the difference has increased to 0.0050 (fig. 15). Although there was a small difference in leading-edge camber (described previously) for these two configurations, unpublished tests indicate that it has a minor effect on the drag due to lift. The F-102A model had lower drag at Mach numbers above about 0.95 than the modified-wing F-102 of reference 5 but a higher drag at lower Mach numbers. With respect to the original F-102 (ref. 4), the F-102A had decreased drag at lift coefficients above approximately 0.15 throughout the speed range.

The maximum lift-drag ratios for the F-102A decreased from 10.6 at a Mach number of 0.60 to 6.2 at a Mach number of 1.075 whereas the lift coefficients at which the maximum lift-drag ratios occurred increased from 0.22 to 0.31 over the same Mach number range (fig. 16). As would

be expected, the maximum lift-drag ratios for the F-102A were increased about 15 to 25 percent with respect to the original F-102 (ref. 4). However, in the Mach number range below 0.95, the F-102A had about 15 percent lower maximum lift-drag ratios than did the modified-wing F-102 of reference 5.

Lift and Pitching-Moment Characteristics

The lift-curve slope for the F-102A increased from 0.045 at a Mach number of 0.60 to a peak of 0.058 at a Mach number of 1.06 (fig. 17) and in general was slightly higher than for the previous versions of the F-102 compared herein.

The pitching-moment curves indicate a region of near neutral stability with possible pitch-up tendencies for the F-102A at high subsonic Mach numbers and at lift coefficients generally between 0.4 and 0.5 (fig. 9(c)). As stated in reference 5, this neutral stability was an effect introduced by the addition of leading-edge camber; the chord-wise fences which essentially eliminated the pitch-up tendency on the plane-wing F-102 (see ref. 1) were not adequate for the cambered wing.

The value of the static-longitudinal-stability parameter $\partial C_m / \partial C_L$ decreased from -0.075 at a Mach number of 0.60 to -0.185 at 1.075, indicating an 11-percent rearward shift of the aerodynamic-center location for the F-102A in the transonic range (fig. 17). Shifts of similar magnitude were indicated for models of references 4 and 5.

CONCLUSIONS

Comparing the results of transonic wind-tunnel tests of a 0.04956-scale model of the Convair F-102A airplane with previous transonic wind-tunnel results for the original Convair F-102 and a modified-wing version of the F-102 indicated the following conclusions:

1. Fuselage indentation and extension employed on the F-102A decreased the minimum drag-coefficient rise about 25 percent between the Mach numbers of 0.85 and 1.075 with respect to the original F-102; the wing modifications and increased surface area for the F-102A increased its drag-coefficient level about 0.0020 at a Mach number of 0.85. With respect to the modified-wing F-102, the F-102A had a 25 percent lower drag-coefficient rise but a 0.0010 higher subsonic drag-coefficient level.
2. The cambered leading edges and deflected tips on the F-102A as for the modified wing F-102 were responsible for sizeable reductions

°°
 ,°°°
 ,°°°
 °°°°
 °°°°
 °°°°
 °°

in drag at lifting conditions when compared with the original (plane-wing) F-102. The F-102A had 15 to 25 percent higher maximum lift-drag ratios than did the original F-102. The F-102A had slightly higher maximum lift-drag ratios than the modified-wing F-102 at Mach numbers above 0.95; however, the F-102A had about 15 percent lower maximum lift-drag ratios at lower Mach numbers indicating an adverse effect of the body modifications on drag at lift at subsonic speeds.

3. The lift characteristics of the F-102A were similar to the earlier F-102 configurations. Chordwise wing fences which provided suitable longitudinal stability for the original plane-wing F-102 were not adequate for the cambered-wing F-102A. The pitching-moment curves indicated a region of near neutral stability with possible pitch-up tendencies for the F-102A at high subsonic speeds and at lift coefficients between approximately 0.4 and 0.5.

Langley Aeronautical Laboratory,
 National Advisory Committee for Aeronautics,
 Langley Field, Va., March 28, 1955.

Robert S. Osborne
 for
 Kenneth E. Tempelmeyer
 Aeronautical Research Scientist

Robert S. Osborne
 Robert S. Osborne
 Aeronautical Research Scientist

Approved:

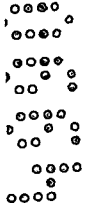
Eugene C. Draley
 Eugene C. Draley
 Chief of Full Scale Research Division

mgk

~~CONFIDENTIAL~~

REFERENCES

1. Osborne, Robert S., and Wornom, Dewey E.: Aerodynamic Characteristics Including Effects of Wing Fixes of a 1/20-Scale Model of the Convair F-102 Airplane at Transonic Speeds. NACA RM SL54C23, U. S. Air Force, 1954.
2. Osborne, Robert S., and Tempelmeyer, Kenneth E.: Longitudinal Control Characteristics of a 1/20-Scale Model of the Convair F-102 Airplane at Transonic Speeds. NACA RM SL54G15, U. S. Air Force, 1954.
3. Wornom, Dewey E., and Osborne, Robert S.: Effects of Body Indentation on the Drag Characteristics of a Delta-Wing—Body Combination at Transonic Speeds. NACA RM L54K12a, 1955.
4. Kelly, Thomas C., and Osborne, Robert S.: Effects of Fuselage Modifications on the Drag Characteristics of a 1/20-Scale Model of the Convair F-102 Airplane at Transonic Speeds. NACA RM SL54K18a, U. S. Air Force, 1954.
5. Tempelmeyer, Kenneth E., and Osborne, Robert S.: Effects of Wing Leading-Edge Camber and Tip Modifications on the Aerodynamic Characteristics of a 1/20-Scale Model of the Convair F-102 Airplane at Transonic Speeds. NACA RM SL54K29, U. S. Air Force, 1954.
6. Carlson, Harry W.: Preliminary Investigation of the Effects of Body Contouring As Specified by the Transonic Area Rule on the Aerodynamic Characteristics of a Delta Wing-Body Combination at Mach Numbers of 1.41 and 2.01. NACA RM L53G03, 1953.
7. Wallskog, Harvey A.: Free-Flight Zero-Lift Drag Results From a 1/5-Scale Model and Several Small-Scale Equivalent Bodies of Revolution of the Convair F-102 Configuration at Mach Numbers up to 1.34. NACA RM SL54D09b, U. S. Air Force, 1954.
8. Spearman, M. Leroy, and Hughes, William C.: Aerodynamic Characteristics at a Mach Number of 1.41 of a Model of the Convair F-102 Airplane Equipped with an Extended Contoured Afterbody, Cambered Wing Leading Edge, and Reflexed Wing-Tip Trailing Edge. NACA RM SL54J26, U. S. Air Force, 1954.
9. Wallskog, Harvey A.: Summary of Free-Flight Zero-Lift Drag Results From Tests of 1/5-Scale Models of the Convair YF-102 and F-102A Airplanes and Several Related Small Equivalent Bodies at Mach Numbers From 0.70 to 1.46. NACA RM SL54J25, U. S. Air Force, 1954.



10. Ritchie, Virgil S., and Pearson, Albin O.: Calibration of the Slotted Test Section of the Langley 8-Foot Transonic Tunnel and Preliminary Experimental Investigation of Boundary-Reflected Disturbances. NACA RM L51K14, 1952.
11. Whitcomb, Richard T., and Fischetti, Thomas L.: Development of a Supersonic Area Rule and an Application to the Design of a Wing-Body Combination Having High Lift-to-Drag Ratios. NACA RM L53H31a, 1953.
12. Nelson, Robert L., and Stoney, William E., Jr.: Pressure Drag of Bodies at Mach Numbers up to 2.0. NACA RM L53I22c, 1953.

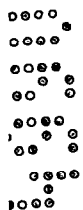


TABLE I

DIMENSIONS OF THE 0.04956-SCALE MODEL OF THE F-102A AIRPLANE

Wing:

Airfoil section . . .	Modified NACA 0004-65 with leading-edge camber	
Total area, sq ft . . .		1.709
Aspect ratio . . .		2.1
Taper ratio . . .		0
Incidence . . .		0
Dihedral . . .		0

Vertical tail:

Airfoil section . . .	Modified NACA 0004-65	
Exposed area, sq ft . . .		0.1704
Aspect ratio . . .		1.1
Taper ratio . . .		0

Fuselage:

Length, in.		34.161
Frontal area (less canopy), sq in.		11.90
Fineness ratio (less canopy).		8.75
Total base area, sq ft		0.0236

Equivalent body of revolution (ducts closed):

For M = 1.0 -

Body length, in.		34.161
Maximum cross-sectional area, sq in.		15.0
Fineness ratio		7.8

For M = 1.2 -

Body length, in.		34.161
Maximum cross-sectional area, sq in.		14.8
Fineness ratio		8.0

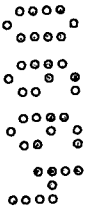
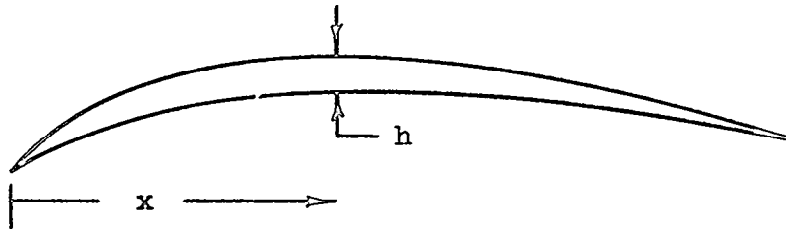


TABLE II

HEIGHT OF CAMBERED-WING FENCE ABOVE WING UPPER SURFACE

[All dimensions in inches]



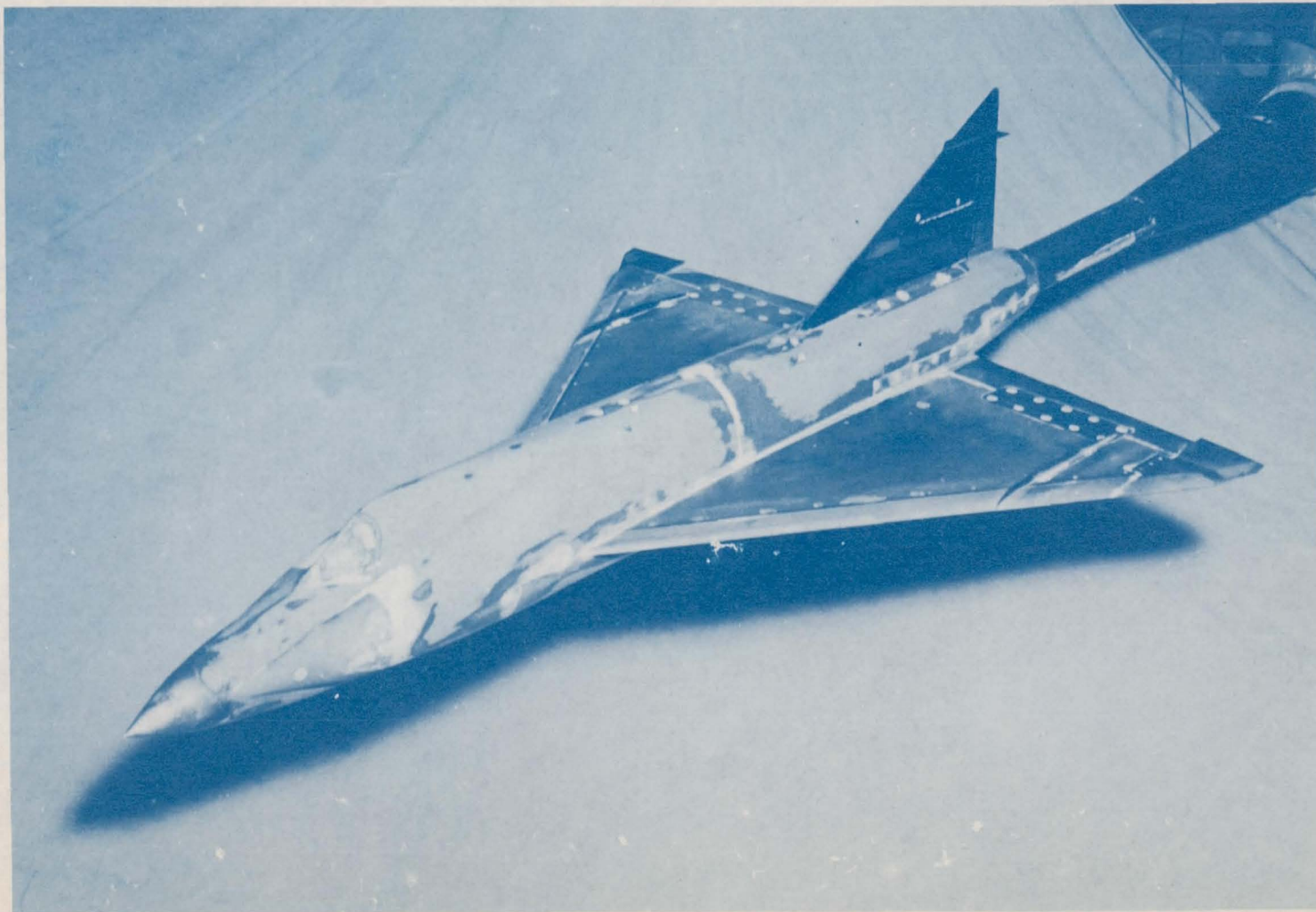
x	h
0	0
.1	.11
.2	.14
.3	.17
.4	.18
.5	.19
.6	.20
.7	.21
.8	.22
.9	.22
1.1	.23
1.3	.23
1.5	.24
1.7	.25
1.9	.26
2.1	.27
2.3	.27
2.5	.27

x	h
2.7	0.27
2.9	.27
3.1	.26
3.3	.25
3.5	.24
3.7	.22
3.9	.20
4.1	.18
4.3	.16
4.5	.15
4.7	.13
4.9	.12
5.1	.11
5.3	.08
5.5	.06
5.7	.03
5.95	0



NACA RM SL55D19

CONFIDENTIAL



L-82280

Figure 1.- Photograph of the 0.04956-scale model of the Convair F-102A airplane tested in the Langley 8-foot transonic tunnel.

CONFIDENTIAL

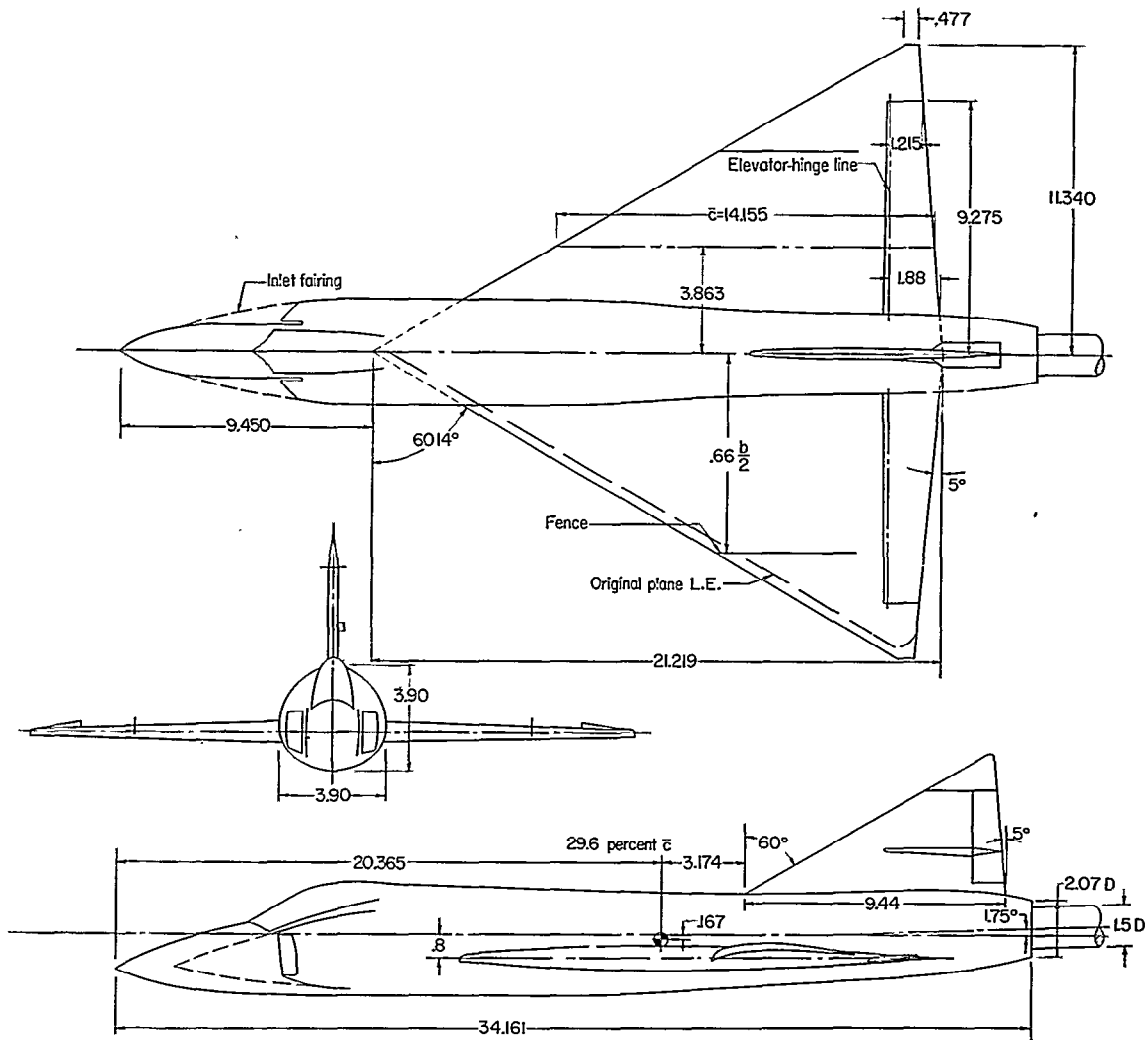
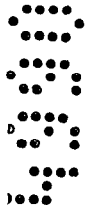
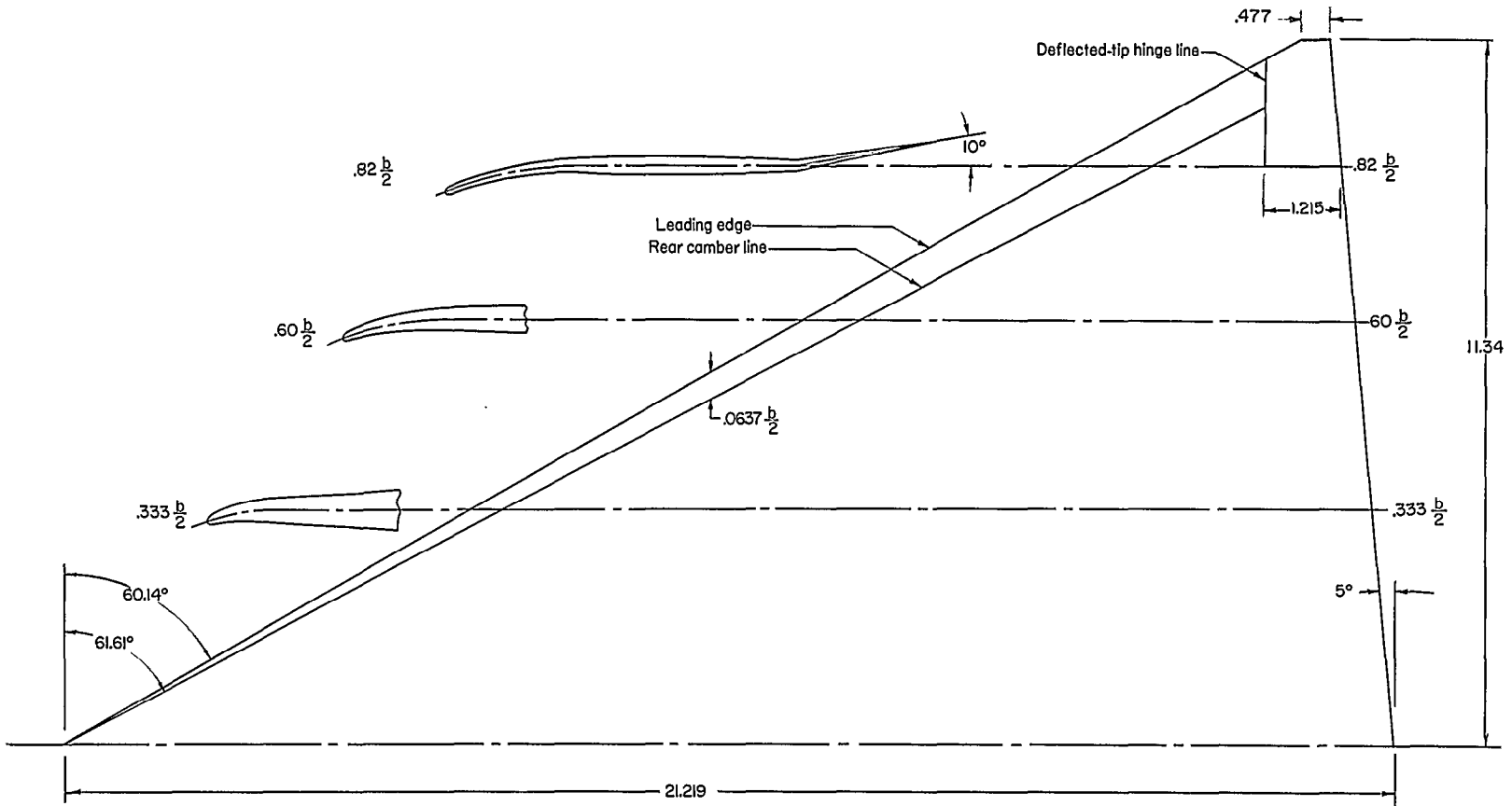
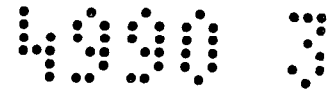


Figure 2.- Model details. All dimensions are in inches unless otherwise noted.



Plan form and streamwise airfoil sections not to same scale

Figure 3.- Dimensional details of the leading-edge camber and F-102A plan form. All dimensions in inches unless otherwise noted.

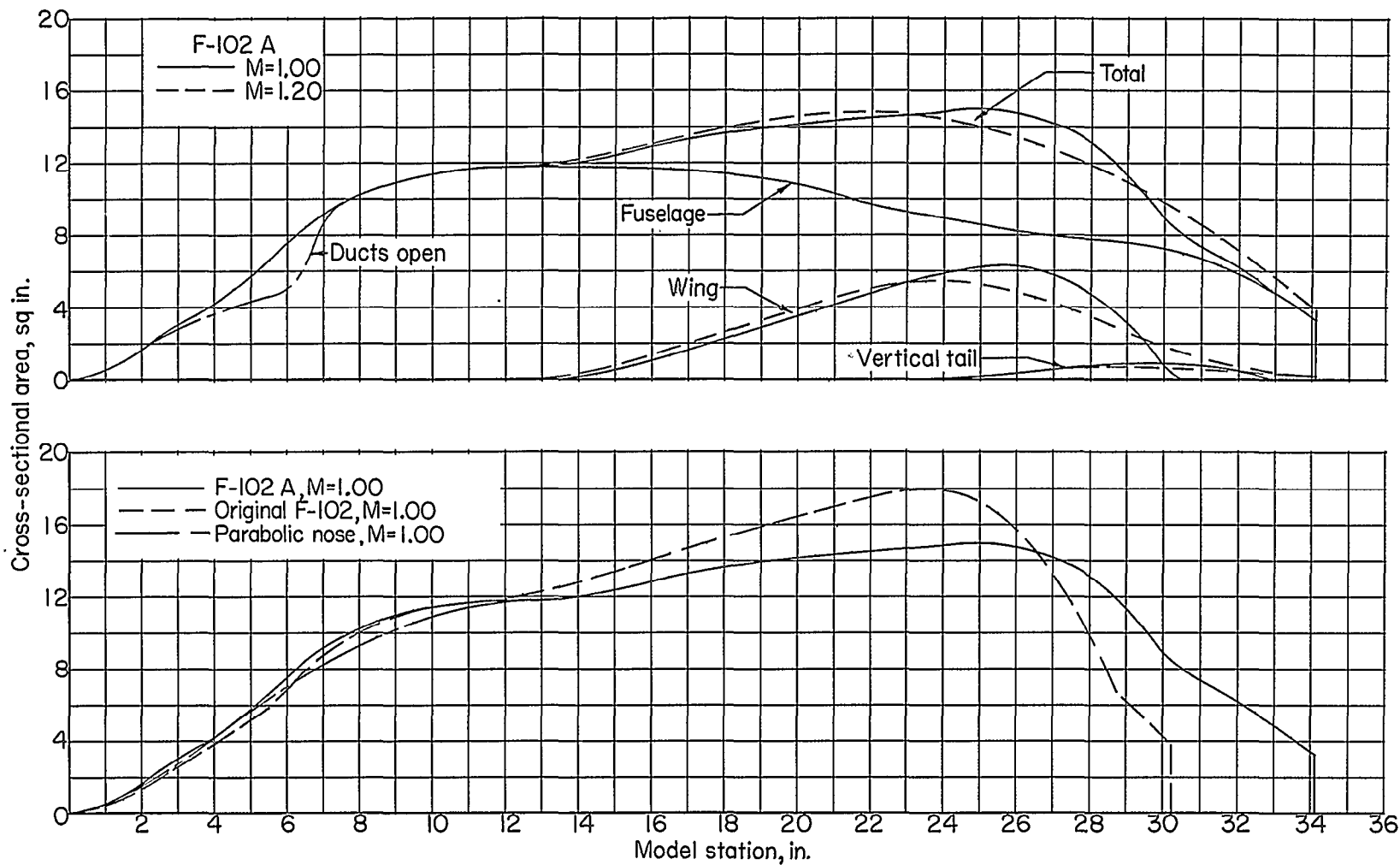
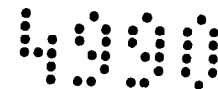


Figure 4.- Axial variation of the cross-sectional area distribution for the Convair F-102A and F-102 airplanes.

500

MACA RM SL55D19

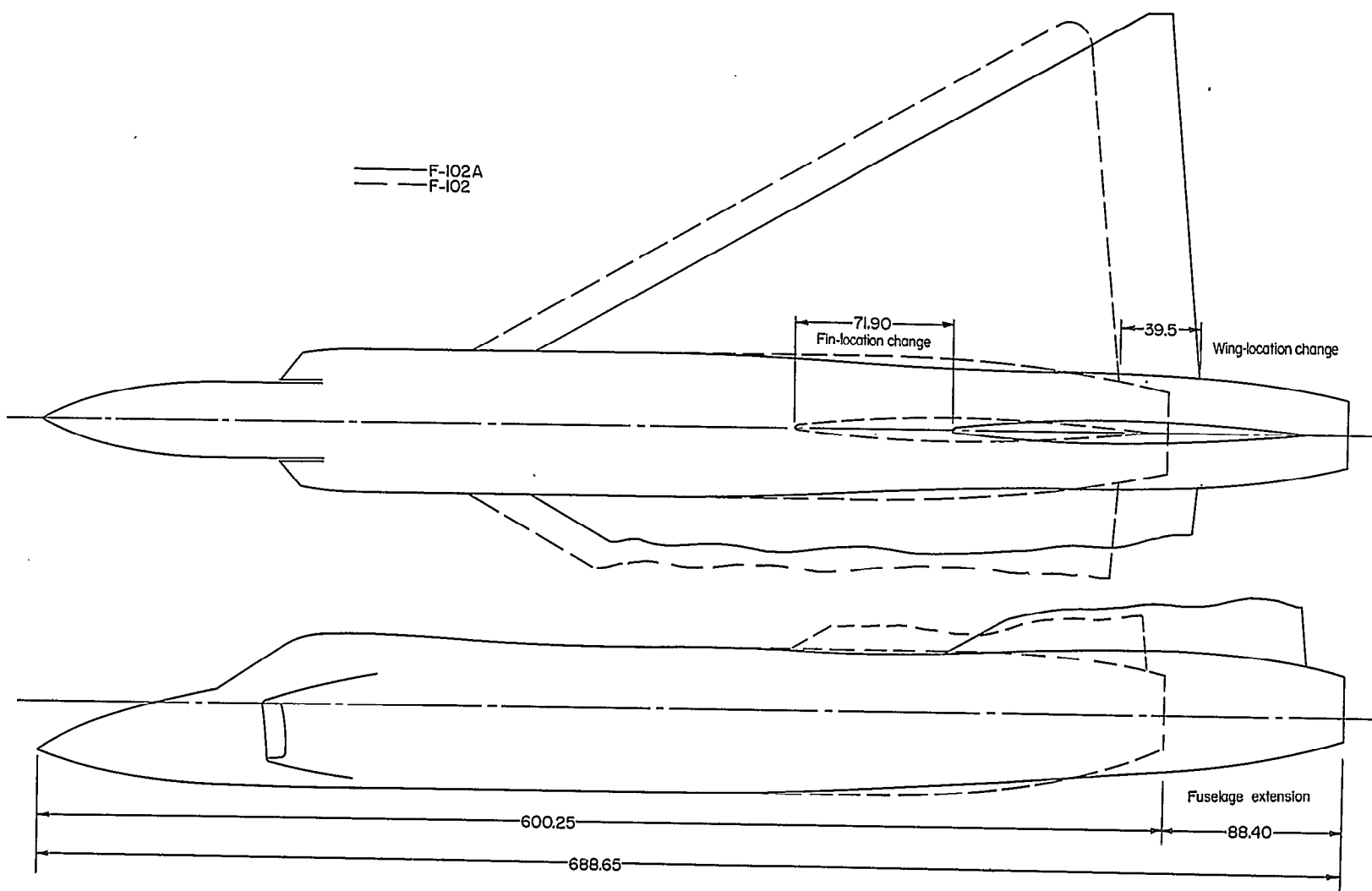


Figure 5.- Comparison of the full-scale Convair F-102A and the F-102.
All dimensions are in inches.

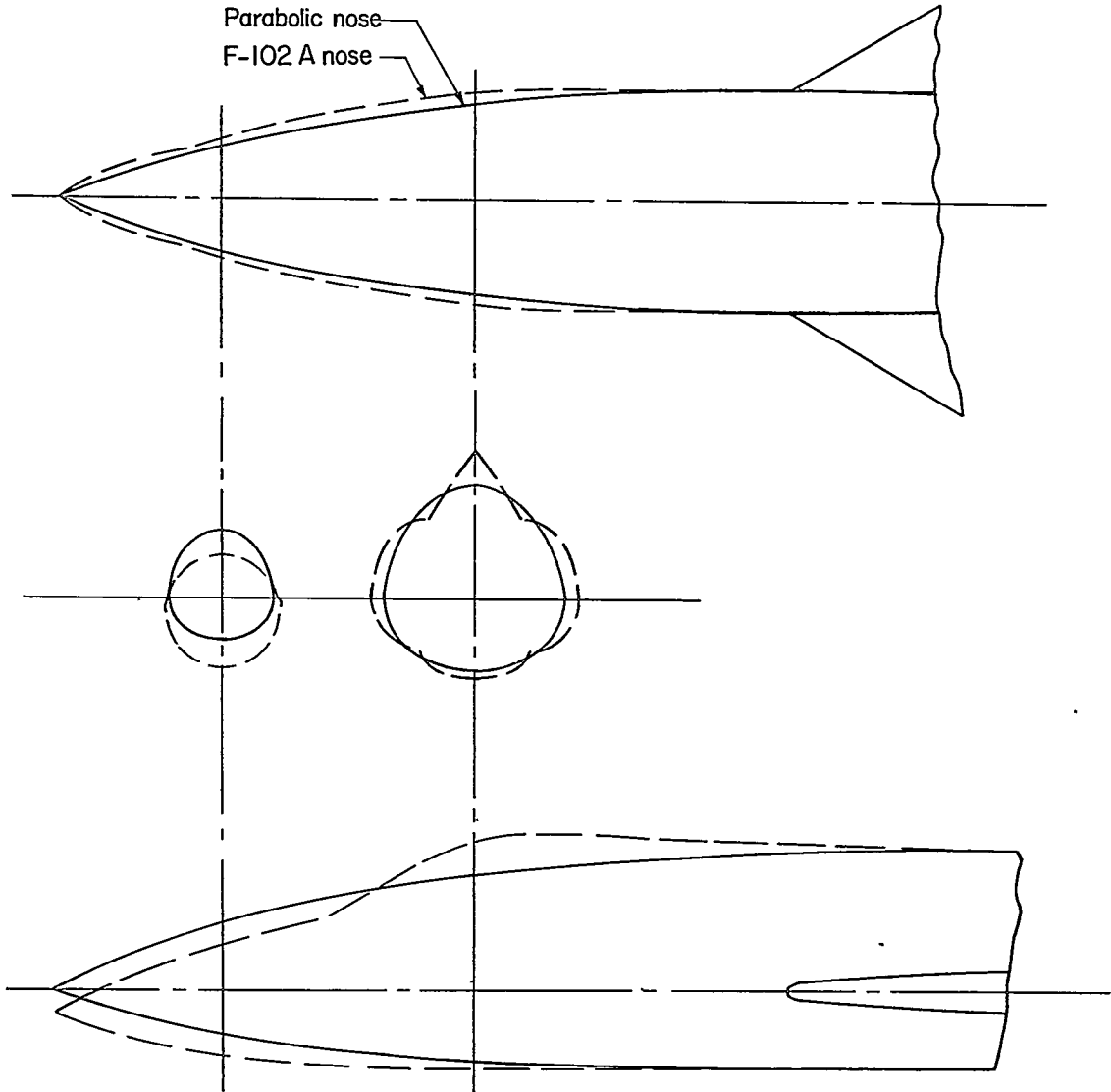
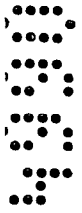


Figure 6.- Comparison of the parabolic nose and the F-102A nose.

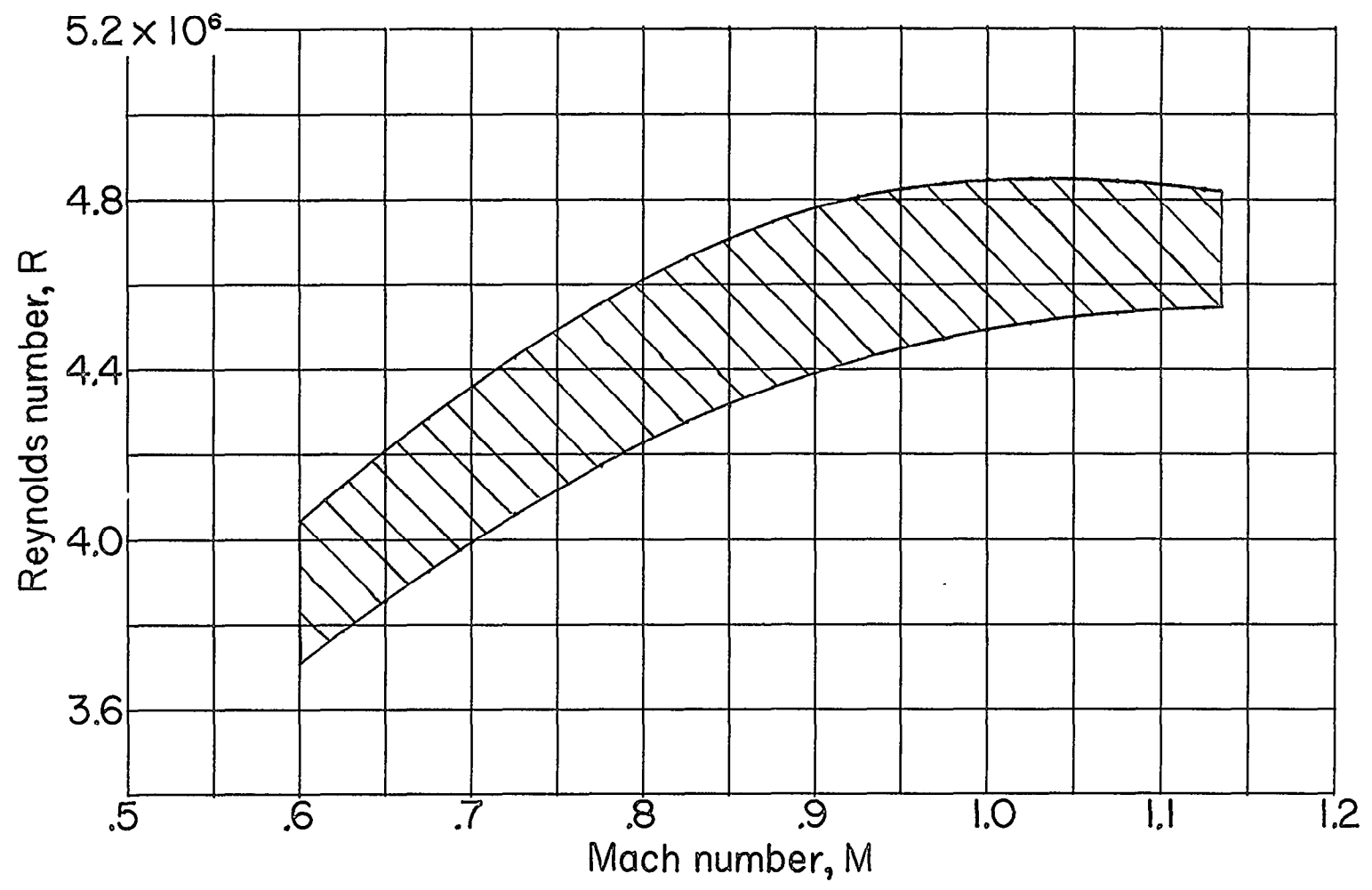
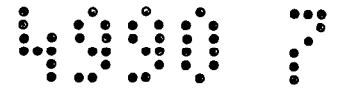


Figure 7.- Variation with Mach number of test Reynolds number based on mean aerodynamic chords.

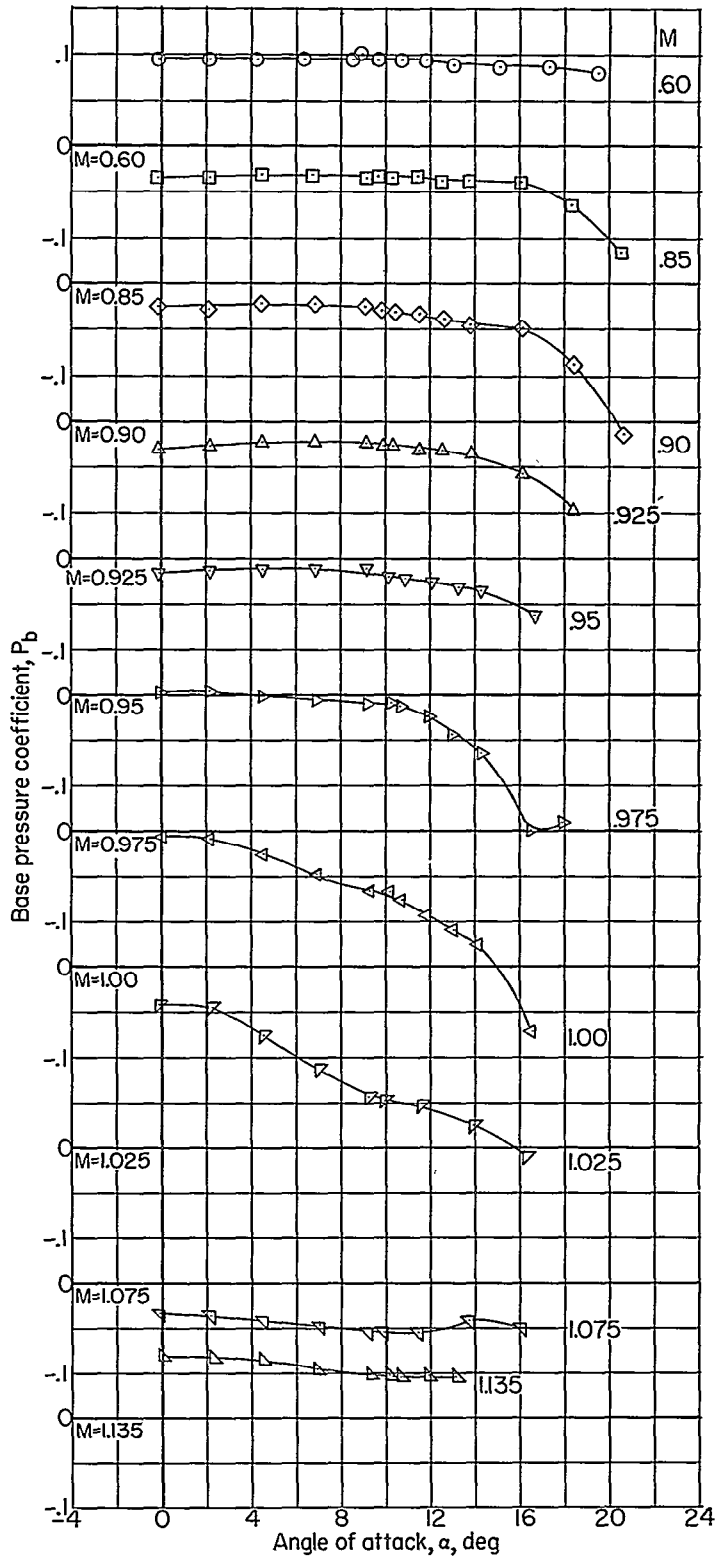
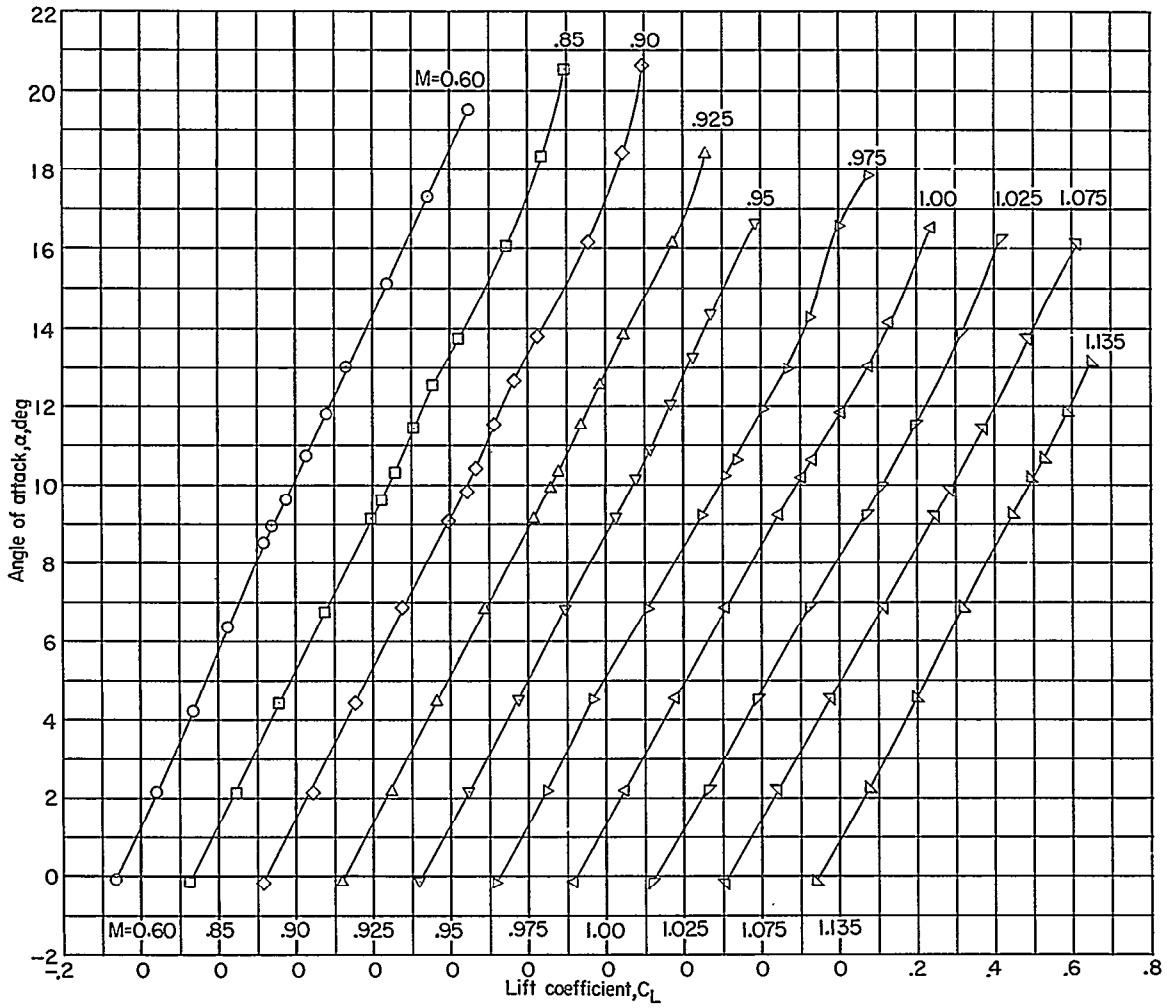
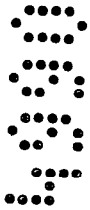
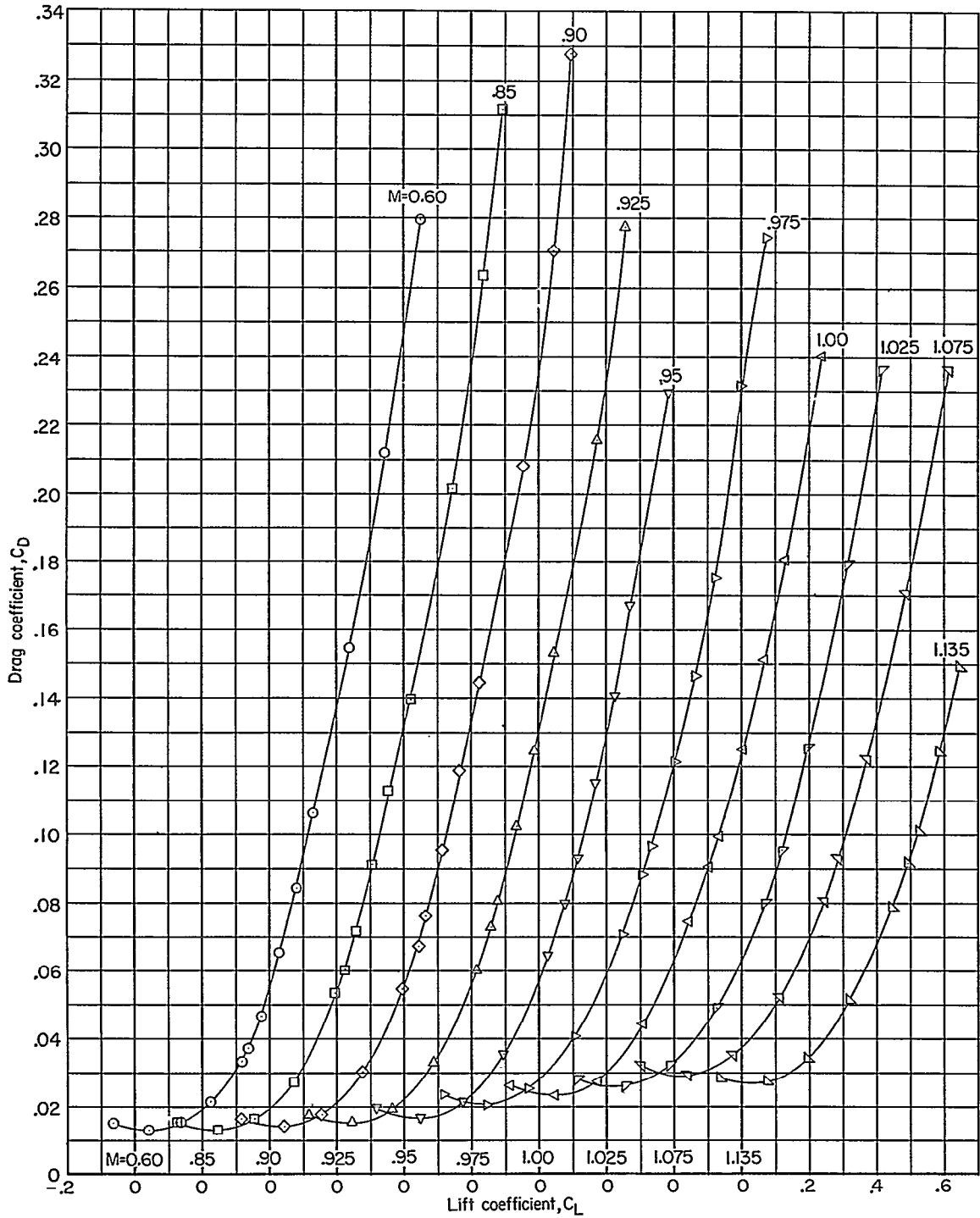


Figure 8.- Base pressure coefficients for the F-102A model.



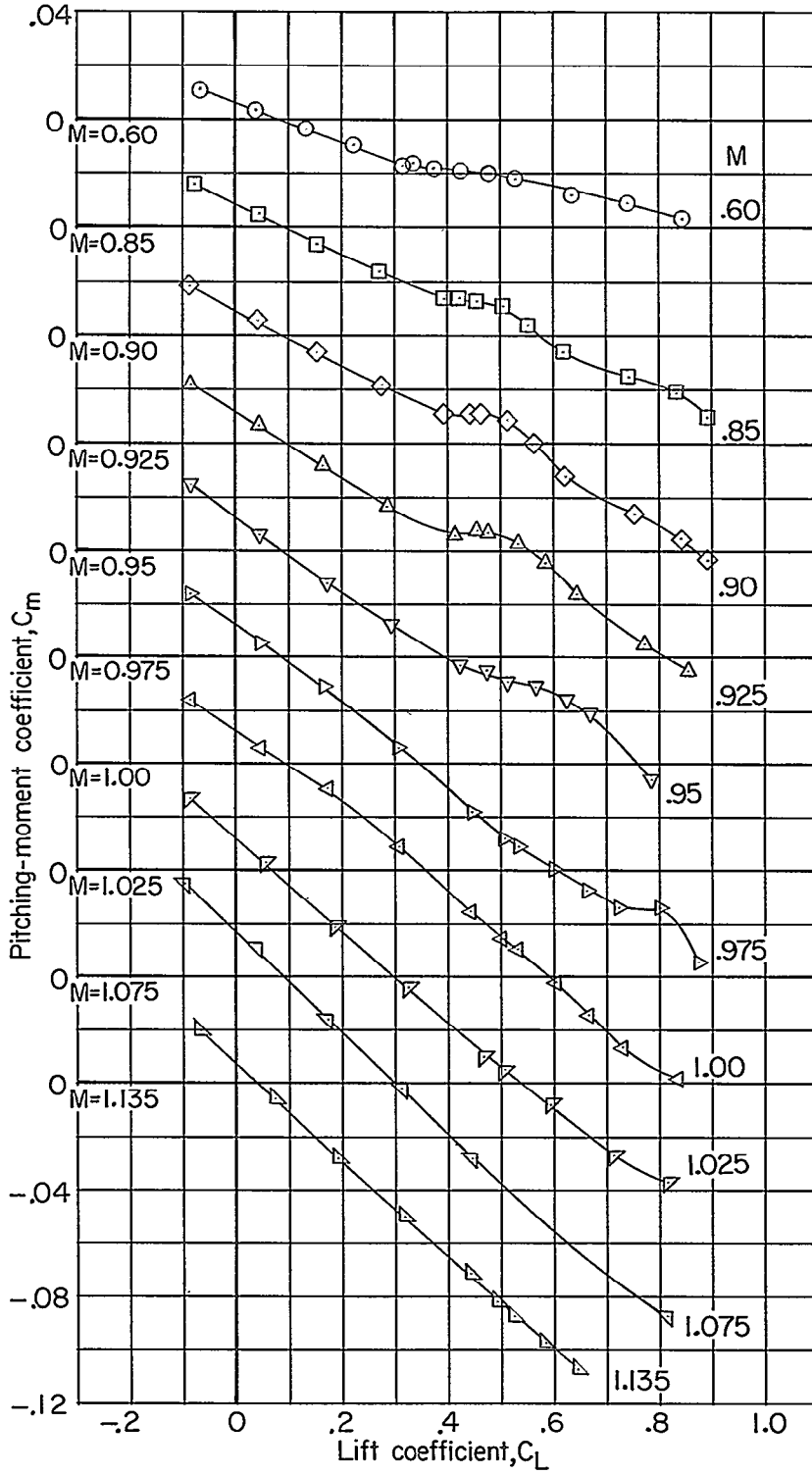
(b) Lift.

Figure 9.- Continued.



(a) Drag.

Figure 9.- Force and moment characteristics for the basic Convair F-102A model.



(c) Pitching moment.

Figure 9.- Concluded.

10000

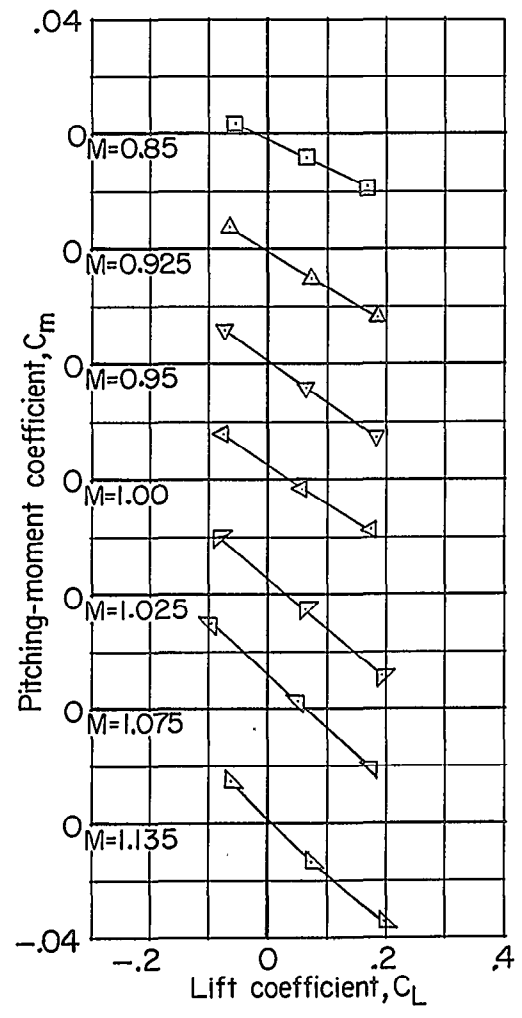
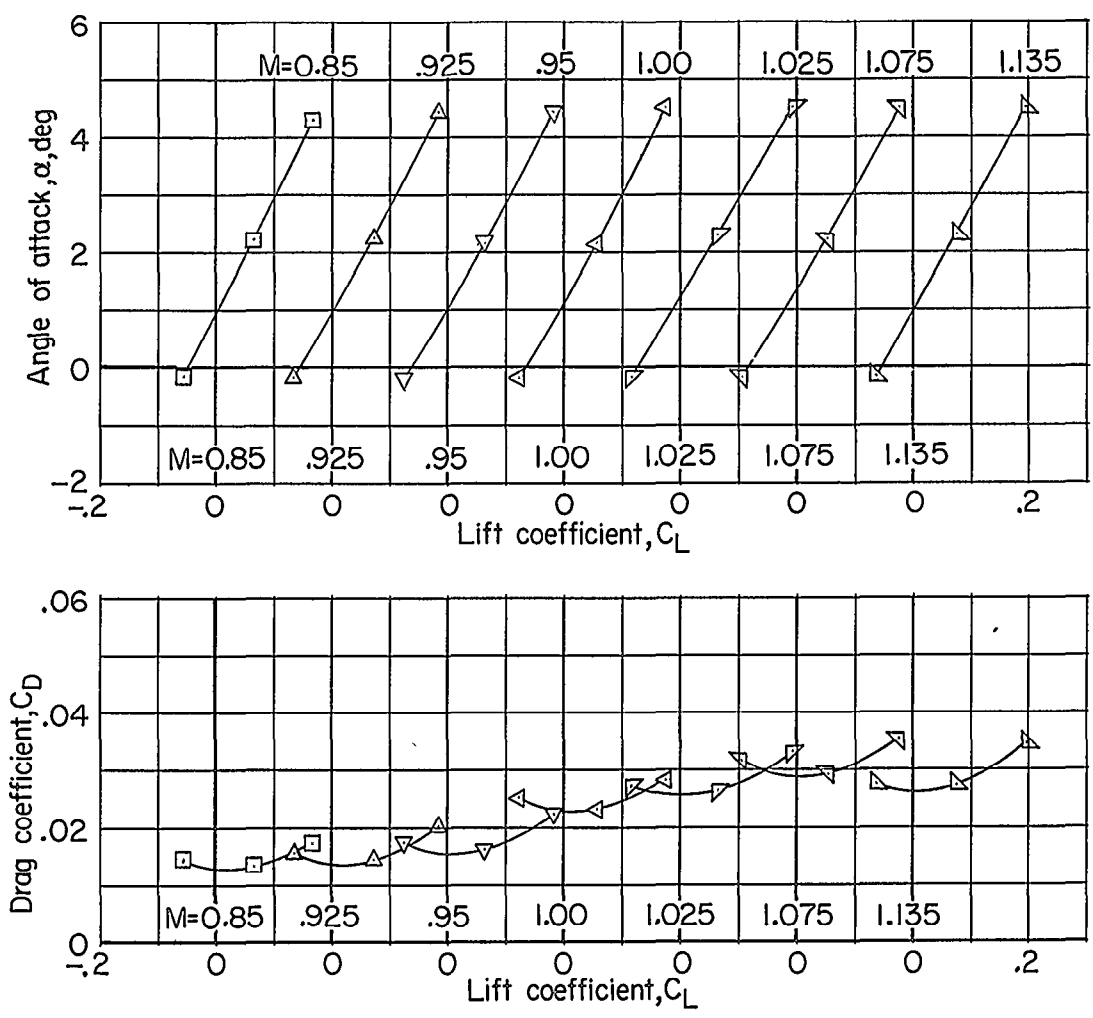


Figure 10.- Force and moment characteristics for the Convair F-102A model with tips undeflected.

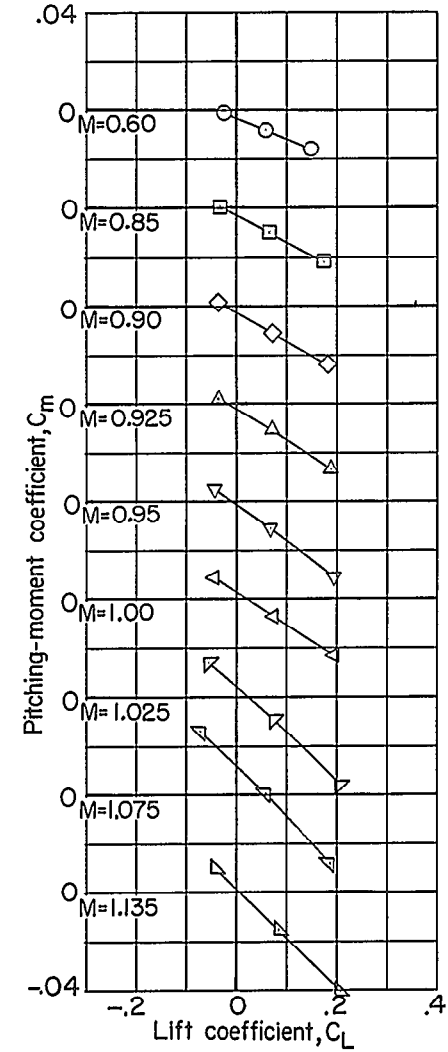
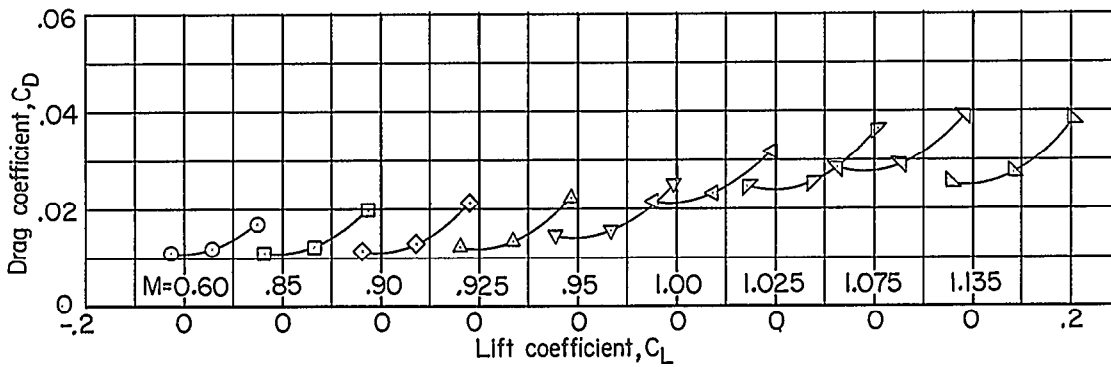
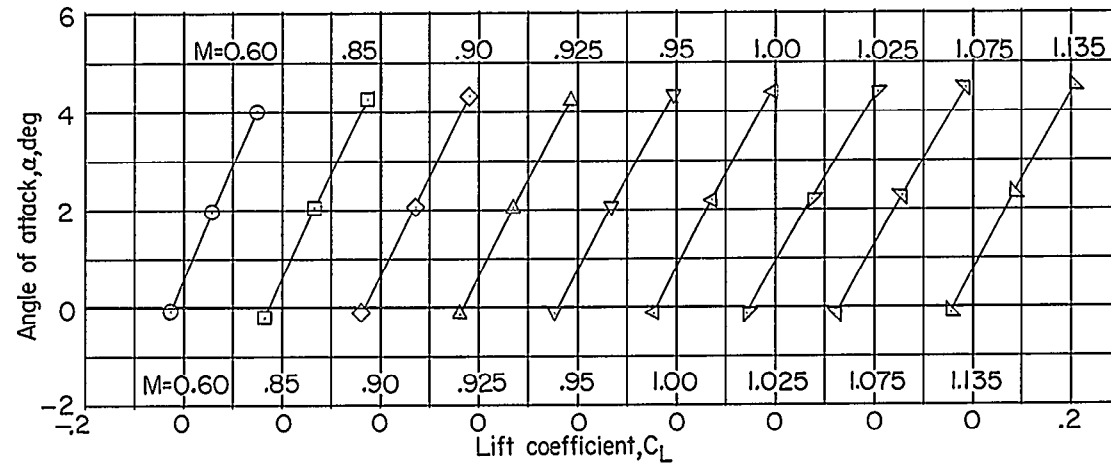


Figure 11.- Force and moment characteristics of the F-102A with plane leading edges and undeflected tips.

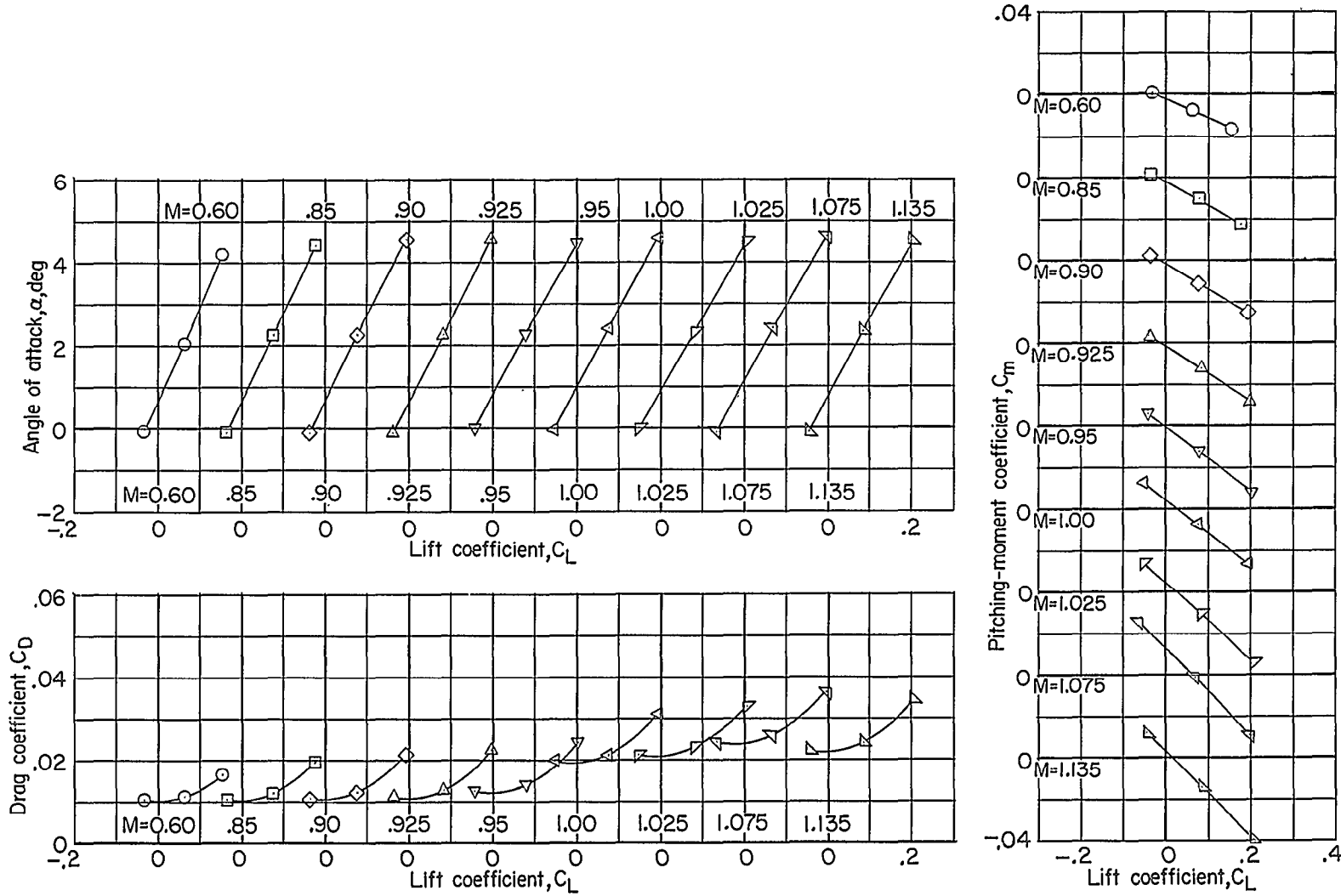
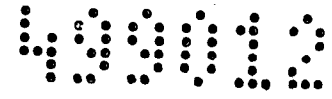


Figure 12.- Force and moment characteristics of the F-102A with a parabolic nose, plane leading edges, and undeflected tips.

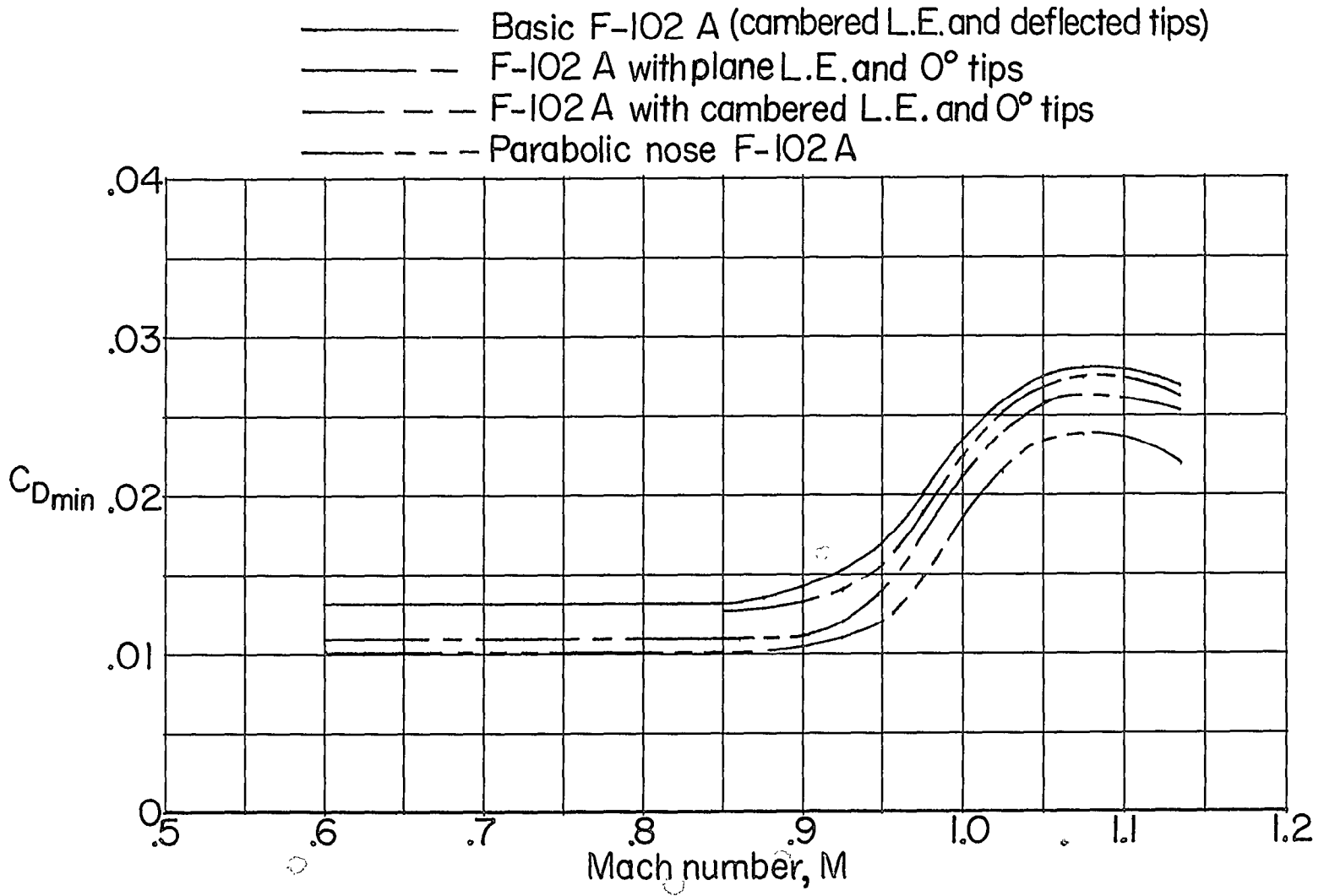


Figure 13.- Effects of leading-edge camber, deflected tips, and a parabolic nose on the minimum drag coefficient.

4001

MACA RM SLS5D19

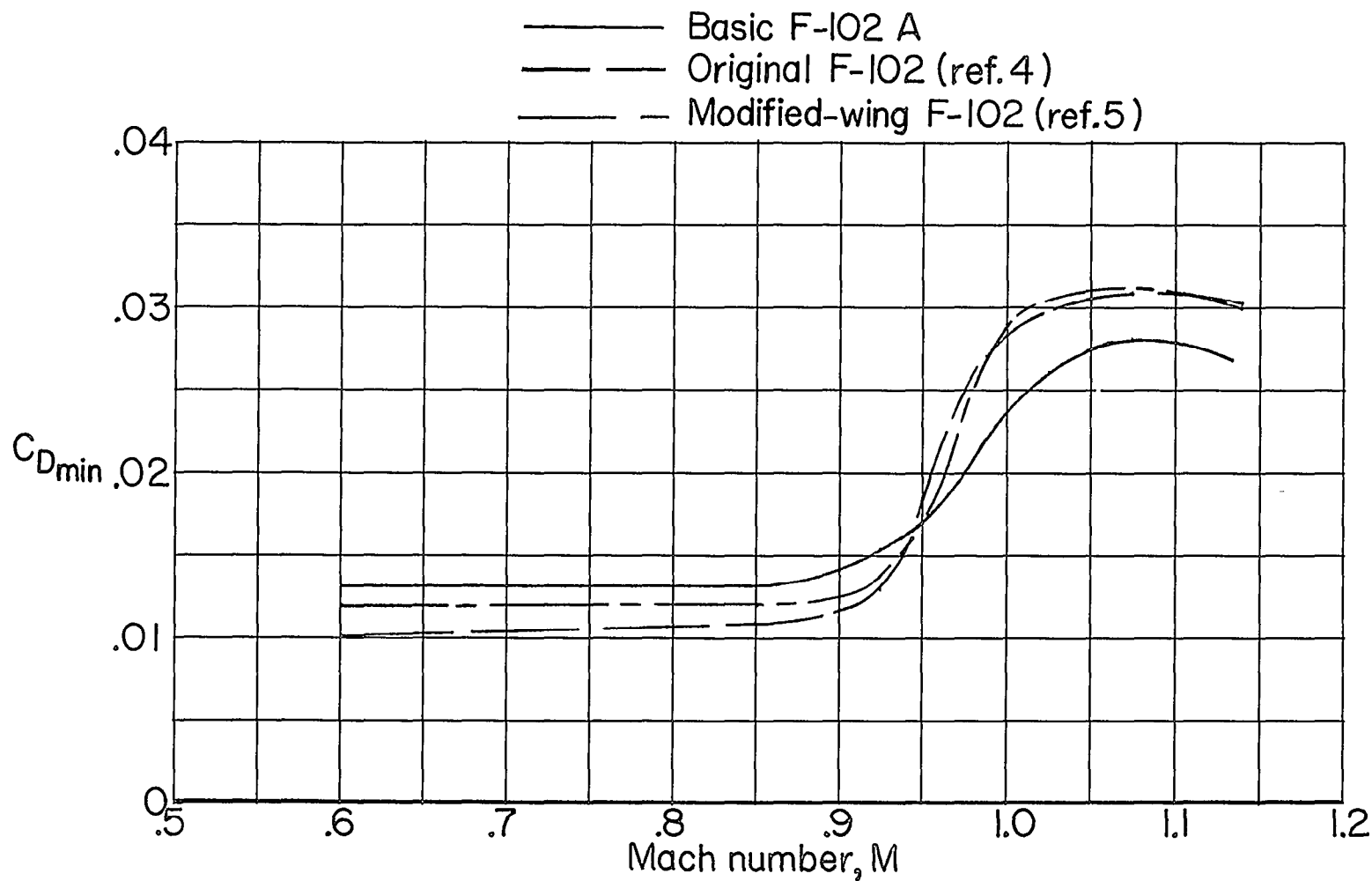


Figure 14.- Minimum drag coefficient of the F-102A compared with that for the original F-102 and the modified-wing F-102.

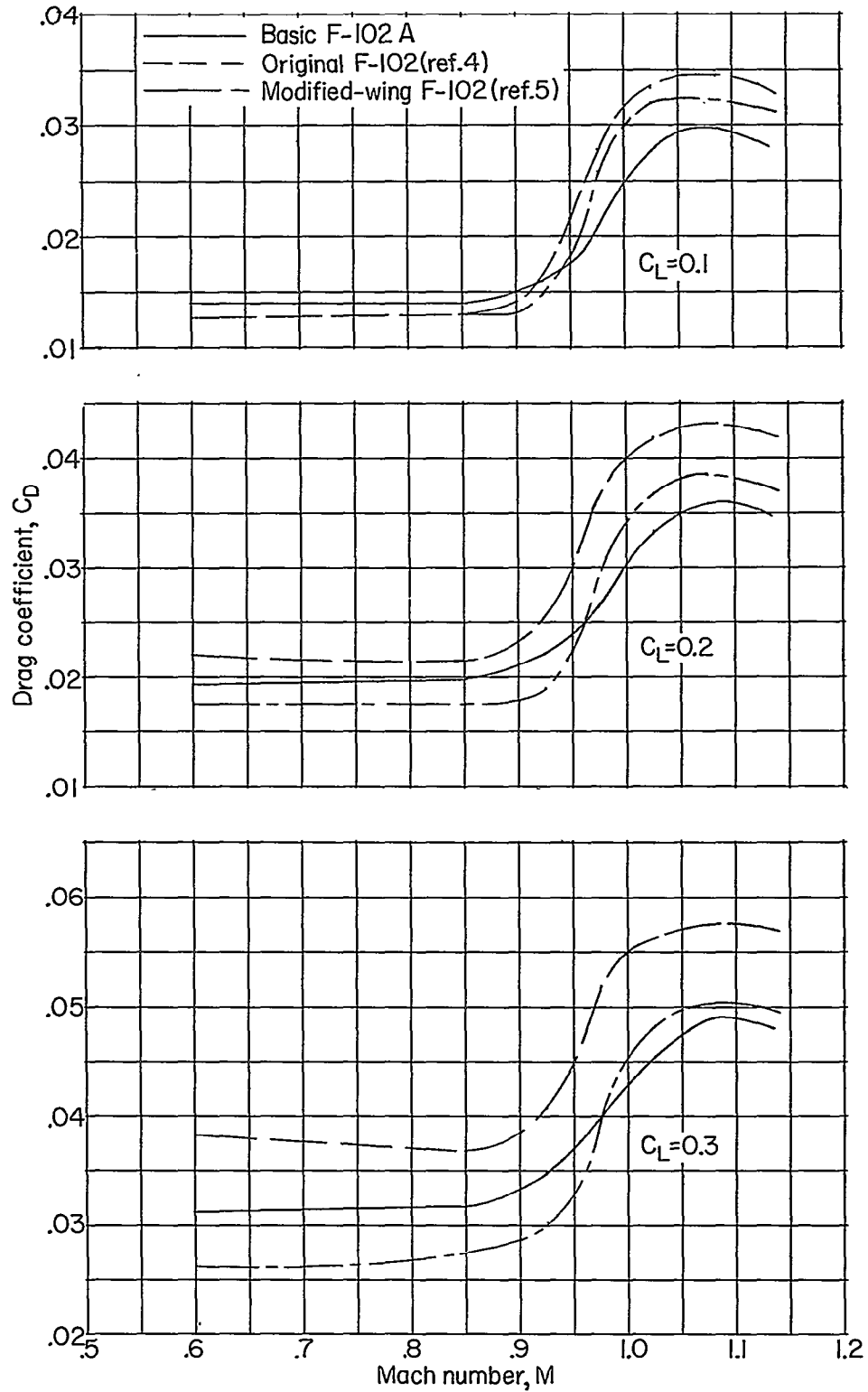
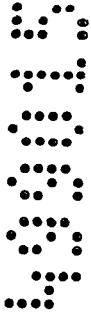


Figure 15.- Drag coefficients at lifting conditions of the F-102A compared with those for the original F-102 and the modified-wing F-102.

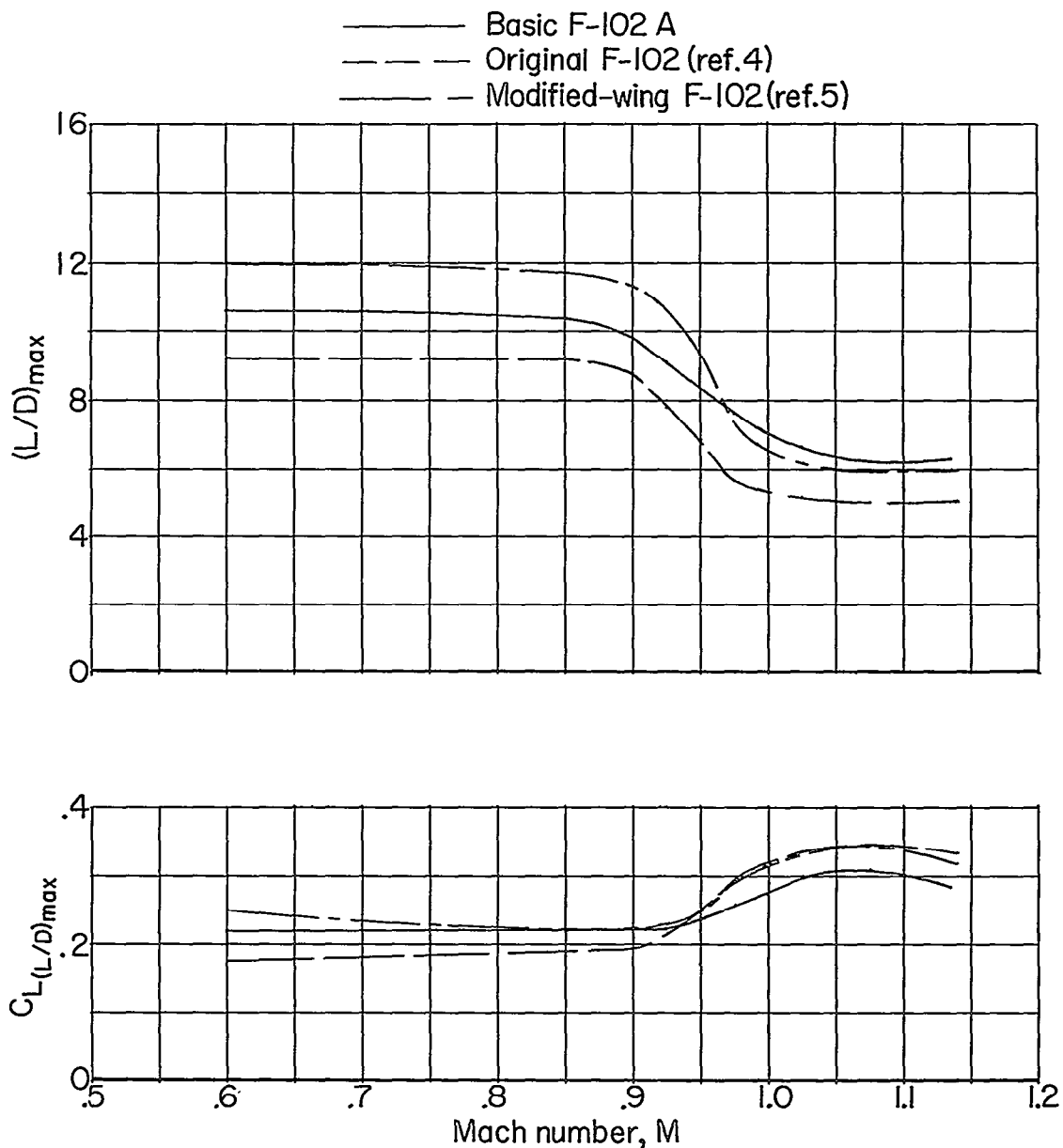
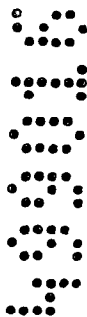


Figure 16.- Maximum lift-drag ratio characteristics of the F-102A compared with those for the original F-102 and the modified-wing F-102.

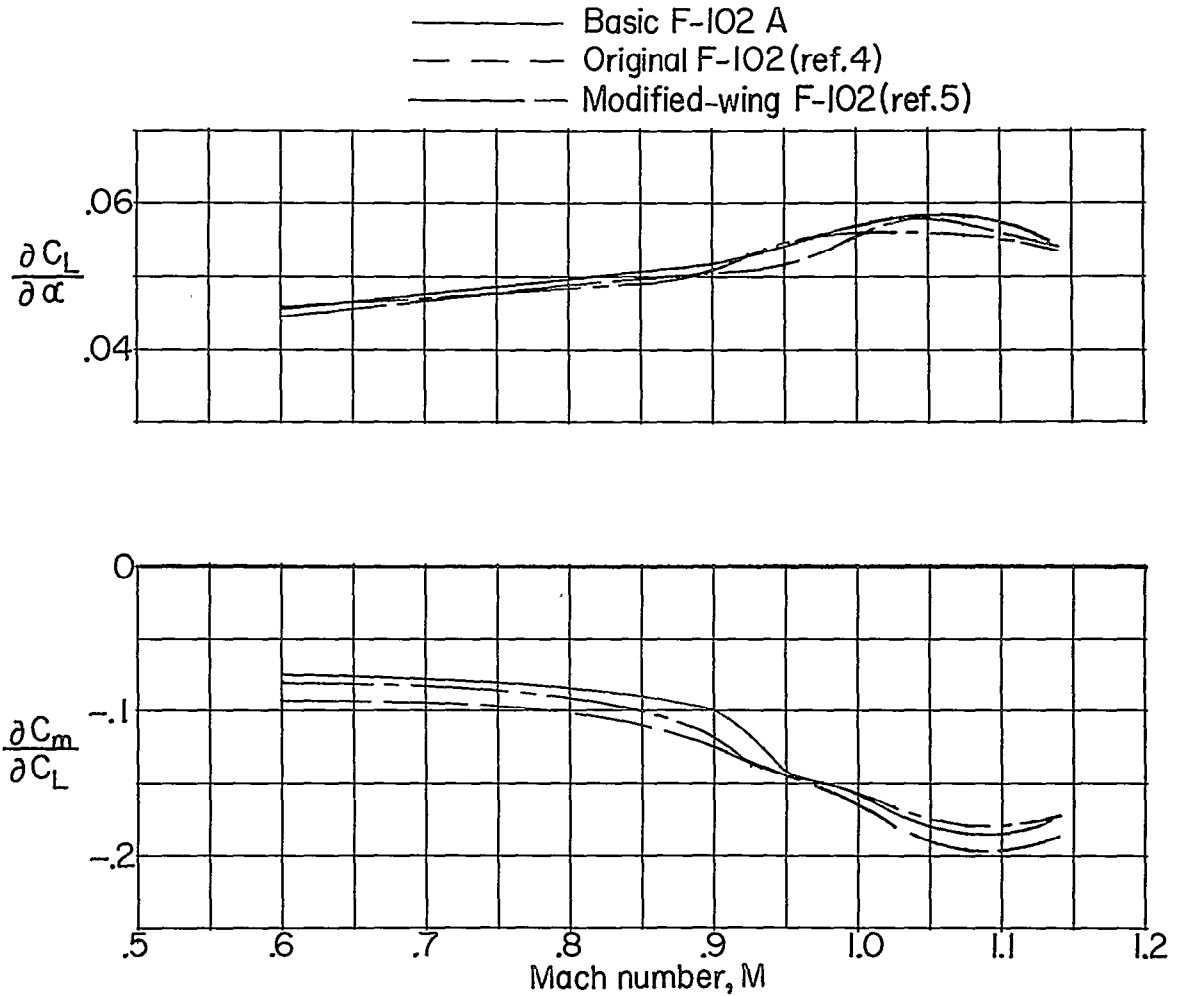
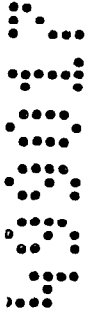
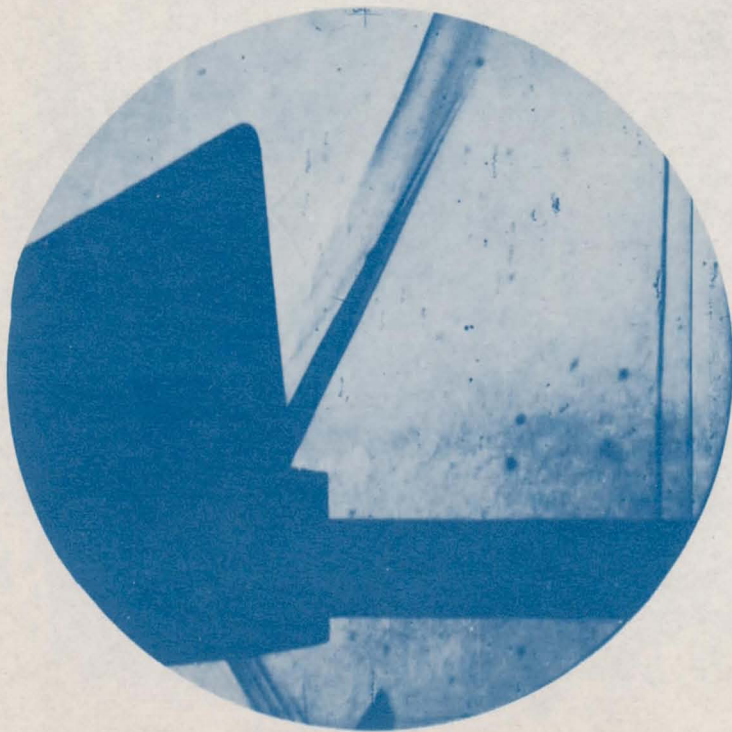
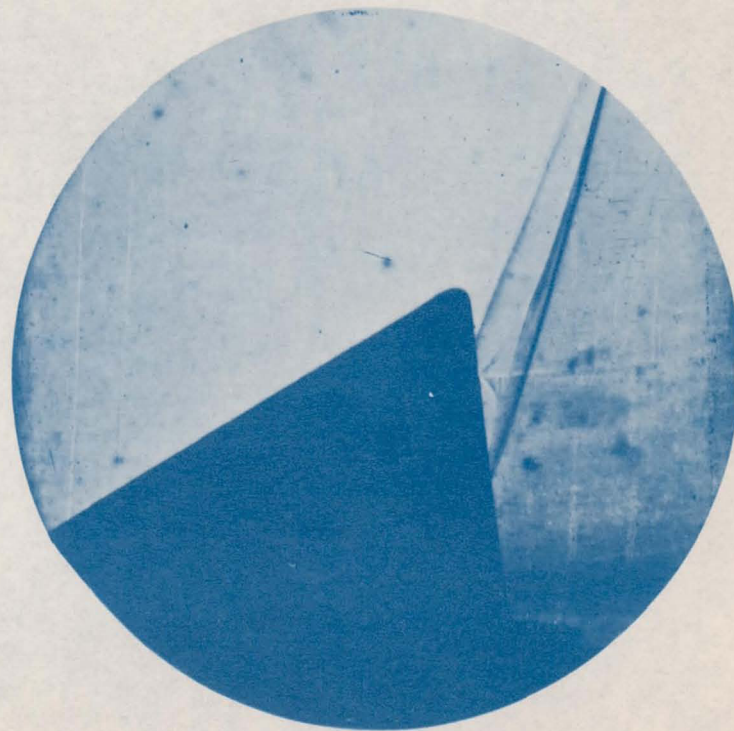


Figure 17.- Lift-curve slope and the static-longitudinal-stability parameter of the F-102A compared with those for the original F-102 and the modified-wing F-102.



Original F-102 (ref.4)



F-102 A with plane L.E.
and 0° tips

L-87928

Figure 18.- Schlieren photographs of the Convair F-102 and F-102A at a Mach number of 1.0 and at an angle of attack of 0°.